CSIRO Publishing

Publications of the Astronomical Society of Australia

VOLUME 18, 2001

An international journal of astronomy and astrophysics

For editorial enquiries and manuscripts, please contact:
The Editor, PASA,
ATNF, CSIRO,
PO Box 76,
Epping, NSW 1710, Australia
Telephone: +61 2 9372 4590
Fax: +61 2 9372 4310
Email: Michelle.Storey@atnf.csiro.au

For general enquiries and subscriptions, please contact:
CSIRO Publishing
PO Box 1139 (150 Oxford St)
Collingwood, Vic. 3066, Australia
Telephone: +61 3 9662 7666
Fax: +61 3 9662 7555
Email: pasa@publish.csiro.au

Published by CSIRO Publishing
for the Astronomical Society of Australia

www.publish.csiro.au/journals/pasa

Publ. Astron. Soc. Aust., 2001, 18, 267–280

Relativistic Jet Flow from a One Dimensional Magnetic Nozzle — Analytic Solutions

Kurt Liffman

Advanced Fluid Dynamics Laboratory, CSIRO/BCE,
PO Box 56, Highett, Vic 3190, Australia
Kurt.Liffman@csiro.au

Received 2000 July 10, accepted 2001 July 18

Abstract: Magnetohydrodynamic devices that can accelerate plasmas to speeds of the order of hundreds of kilometres per second have been designed and built for nearly forty years. Up to the time of writing, however, the theory for such devices has been exclusively non-relativistic. In this paper we derive the special relativistic magnetohydrodynamic (SRMHD) equations and use them to obtain the relativistic, magnetic nozzle equation which describes the production of jet flows with speeds approaching the speed of light. We obtain analytic solutions to this equation and show that, in principle, magnetic field gradients can accelerate a plasma to highly relativistic speeds. We also show that the exit kinetic energy, E_K, of a particle is given by the equation $E_K = m_0 C_{FR}^2$, where m_0 is the rest mass of the particle and C_{FR} is the fast magnetosonic speed at the start of the flow.

The relativistic nozzle differs in a number of ways from the non-relativistic case. A non-relativistic nozzle has a relatively symmetric converging/diverging shape, while a highly relativistic nozzle converges in the usual manner, but diverges, in an abrupt fashion, at the very end of the nozzle. The gentle divergence of non-relativistic nozzles causes the exit plasma densities and magnetic fields of the flow to have values that are small relative to their values at the start of the nozzle. The abrupt divergence of a highly relativistic nozzle implies that, for a less than perfect nozzle, the exit values of the mass density and the magnetic field strength are comparable to their initial values. This unexpected dichotomy in behaviour may have future application in understanding the 'radio-loud' and 'radio-quiet' relativistic jets that are produced from astrophysical sources.

Keywords: plasmas — relativity — galaxies: jets — stars: winds, outflows

1 Introduction

The magnetohydrodynamic acceleration of electrically conducting fluids was first analysed by Hartmann in the 1930s (Hughes & Brighton 1991). Hartmann's work was the forerunner of plasma acceleration devices that have been used extensively in a number of fields ranging from space-craft propulsion, fusion research and power generation (Sutton & Sherman 1965; Jahn 1968). A major result of this research was the discovery, by A. I. Morozov and his colleagues in the late 1950s, of a class of solutions for magnetically driven flows which were similar to the Hugoniot solution for a de Laval jet (Morozov & Solov'ev 1980; Morozov 1990). Other authors appear to have, independently, obtained this result at a slightly later time (Pai 1962). Morozov's work showed that the signal velocity of the magnetic engine is of the order of the Alfvén speed, C_A. In a standard jet engine the signal velocity is of the order of the sound speed, C_S. For a laboratory, a possible parameterised value of the Alfvén speed is

$$C_A = 282 \left(\frac{B}{0.01\ \mathrm{T}} \right) \left(\frac{10^{-12}\ \mathrm{g\ cm^{-3}}}{\rho} \right)^{1/2} \mathrm{km\ s^{-1}}, \quad (1)$$

where B is the magnetic field strength and ρ is the mass density of the plasma. Equation (1) illustrates the high speed flow characteristics of a magnetic rocket engine. Morozov and his colleagues built working models of these devices. Later in 1963, researchers in the US (Ducati, Giannini & Muehlberger 1964), accidently and independently, also discovered how to build such magnetogasdynamic jet engines (Jahn 1968). This research continues in laboratories around the world, where the current magnetic thrusters produce flow speeds of order $100\ \mathrm{km\ s^{-1}}$ (Schoenberg et al. 1991). While these are impressive speeds, it may be possible for a magnetic jet to obtain speeds of much greater magnitude, since one can change the Alfvén speed to be greater than $100\ \mathrm{km\ s^{-1}}$. In this paper, we examine the consequences of setting C_A to be $\gg c$.

Many of the standard magnetoplasmadynamic (MPD) thrusters have a basic structure schematically shown in Figure 1. Here a flow, $\boldsymbol{v}$, is driven by an electric field, $\boldsymbol{E}$, crossed with a magnetic field, $\boldsymbol{B}$ through a channel of varying cross-section, A.

In the collisionless case, both the positive and negative particles are driven to the same speed and direction down the nozzle (Figure 2). A magnetic nozzle engine is, therefore, a particle accelerator. Of course with a maximum exit speed of order $100\ \mathrm{km\ s^{-1}}$, the current MPD thrusters are irrelevant to the needs of modern particle physics. However, if $C_A \gg c \gg C_S$ then, as we show in Section 4.3, one can obtain a relativistic jet with particle kinetic energies, E_K, given by the equation

$$E_K = m_0 C_{FR}^2 \gg m_0 c^2, \quad (2)$$

10.1071/AS01034 1323-3580/01/03267$05.00

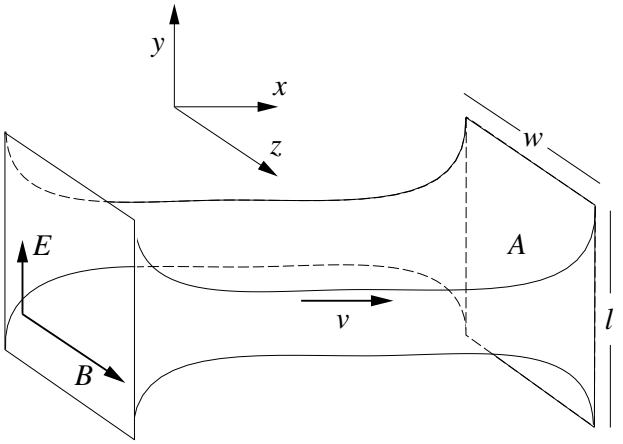

Figure 1 Channel flow with a magnetic field between high permeability pole pieces. An electric field, $\boldsymbol{E}$, is applied, perpendicular to $\boldsymbol{B}$, to drive the flow.

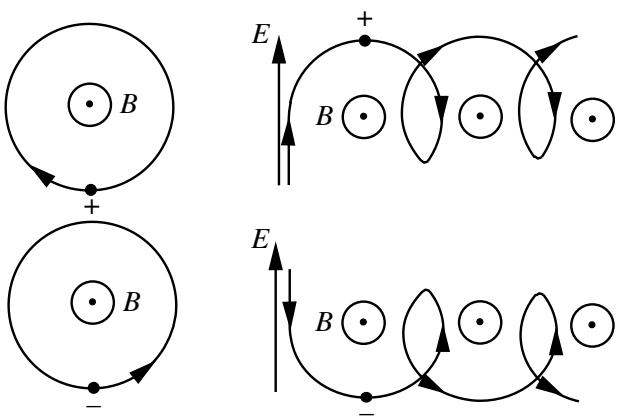

Figure 2 Application of an electric field $\boldsymbol{E}$ perpendicular to a magnetic field $\boldsymbol{B}$ forces positive and negative particles to move in a direction perpendicular to both the electric and magnetic fields. The particles are said to be subject to 'E cross B' drift.

where $C_{FR}\left(=\sqrt{C_{AR}^2+C_{SR}^2}\right)$ is the fast magnetosonic speed at the start of the relativistic jet. Unfortunately, a length scale analysis suggests that a TeV device would be too large to construct with current technology. Nonetheless the theory may have some application for lower energy devices or for understanding the relativistic jets produced by astrophysical sources. In Section 2 we outline the theory for producing a non-relativistic jet from a magnetic nozzle. We do this for ease of reference and pedagogical completeness. The steady state relativistic nozzle equation and its flow constants are derived in Section 3. In Section 4, the behaviour of the flow is examined. We show how, for the highly relativistic case, the nozzle diverges more abruptly at the exit of the flow, and how the exit magnetic field and gas mass density have nearly constant values throughout the nozzle. We also consider some relevant length scales for the relativistic nozzle. Finally, in the Appendices, we derive the special relativistic magnetohydrodynamic equations and the equations for relativistic $\boldsymbol{E}\times\boldsymbol{B}$ drift.

2 The MHD Nozzle Equation

Suppose we have a perfect gas of infinite conductivity flowing with a velocity $\boldsymbol{v}$ through a channel of varying cross-sectional area A (Figure 1). The channel has a constant width, w, a varying height, l, and a magnetic field, $\boldsymbol{B}$, is applied in the $\boldsymbol{z}$ direction. Such a magnetic field 'stiffens' the gas, so that the signal velocity of the medium is now the fast magnetosonic speed. To exploit this property, and to drive the flow, an electric field, $\boldsymbol{E}$, is applied in the $\hat{y}$ direction. For such a configuration, the flow is driven by $\boldsymbol{E}\times\boldsymbol{B}$ drift.

By examining the suitable one dimensional forms of Maxwell's equations and the MHD equations, one can produce (Morozov & Solov'ev 1991; Liffman & Siora 1997) a nozzle equation with the Hugoniot form:

$$\left(\frac{v^2}{C_F^2}-1\right)\frac{1}{v}\frac{dv}{dx}=\frac{1}{A}\frac{dA}{dx}, \tag{3}$$

where v is the x component of $\boldsymbol{v}$, C_F is the fast magnetosonic speed $\left(=\sqrt{C_S^2+C_A^2}\right)$, C_S the sound speed $\left(=\sqrt{\Gamma p/\rho}\right)$, C_A the Alfvén speed $\left(=\sqrt{B^2/(\mu_0\rho)}\right)$, B the magnetic field strength, μ_0 the permeability of free space, ρ the density, p the pressure, and Γ the ratio of specific heats.

If we wish to accelerate the flow ($dv/dx > 0$) then $v^2 < C_F^2 \Rightarrow dA/dx < 0$, i.e. when the flow starts, the nozzle has to converge. Similarly, $v^2 > C_F^2 \Rightarrow dA/dx > 0$, so once we are past the narrowest point in the flow, often called the 'throat', the nozzle must diverge.

Further manipulation of the MHD equations gives the flow constants (Morozov & Solov'ev 1980; Contopoulos 1995; Liffman & Siora 1997)

$$\rho v A = \text{constant}, \tag{4}$$

and

$$BvA = \text{constant}, \tag{5}$$

with an MHD-Bernoulli equation

$$\frac{v^2}{2}+\frac{C_S^2}{\Gamma-1}+C_A^2=\text{constant}. \tag{6}$$

One can use the MHD-Bernoulli equation (Schoenberg et al. 1991; Liffman & Siora 1997) to show that

$$v_E=\sqrt{\frac{2C_{SR}^2}{\Gamma-1}+2C_{AR}^2}=\sqrt{\left[\frac{\Gamma+1}{\Gamma-1}\right]C_{ST}^2+3C_{AT}^2}, \tag{7}$$

where v_E is the exit speed of the nozzle, C_{AT} and C_{ST} are the Alfvén and sound speeds at the throat of the nozzle, while C_{AR} and C_{SR} are the Alfvén and sound speeds at the entrance or 'reservoir' of the nozzle.

https://doi.org/10.1071/AS01034 Published online by Cambridge University Press

In the 'cold' plasma limit ($C_A \gg C_S$) equation (7) reduces to

$$v_E \approx \sqrt{3} C_{AT} = \sqrt{2} C_{AR}, \tag{8}$$

which in turn implies

$$\rho_T = \frac{2}{3}\rho_R \quad \text{and} \quad B_T = \frac{2}{3}B_R, \tag{9}$$

where ρ_T and ρ_R are the gas densities at the throat and reservoir of the nozzle, respectively. Similarly, B_T and B_R refer to the magnetic field strength at the throat and reservoir of the nozzle.

3 The Relativistic Magnetic Nozzle Equation

As a first step in understanding the behaviour of our relativistic jet, we require the ideal special relativistic magnetohydrodynamic (SRMHD) equations. These equations have been slowly revealed in the literature over the last thirty years. Michel (1969) developed a relativistic MHD system to assist in the understanding of relativistic winds (and associated torques) produced from pulsars.Goldreich & Julian (1970), in their study of relativistic stellar winds, added more details to Michel's system including a relativistic continuity equation and the effect of gravity. Landau & Lifshitz (1975) laid out much of the detail for the relevant stress–energy equations, while Kennel, Fujimura & Okamoto (1983), in a very detailed study of relativistic winds, produced an elegant steady state system of SRMHD equations which excluded the effects of gravity. The equations used in this study are just about the same as those developed by Kennel et al. (1983). The most recent, and detailed, listing of the SRMHD equations is to be found in Koide, Nishikawa & Mutel (1996).

In Appendix A we provide a derivation of the Koide et al. equations (with a slightly different notation), illustrating the assumptions involved in obtaining this form of the SRMHD equations. As far as we are aware, such a derivation is not available elsewhere in the literature.

Although we have derived the time dependent SRMHD equations, we concentrate on the steady-state case, since this provides a basic foundation for understanding the formation of relativistic magnetic jet flows, where the flow is perpendicular to the driving magnetic field. Just about all the previous work on relativistic magnetic jet flow has assumed that the flow is parallel to the driving magnetic field. So an illustrative case study using simplified flow equations for this new flow/field configuration is, we believe, a physically reasonable thing to do.

It should be noted that the general relativistic form of the MHD equations has also been developed by a number of authors (e.g. Thorne & Macdonald 1981), but we shall not be discussing the general relativistic case in this paper.

3.1 The Steady-state Relativistic MHD Equations

Our fundamental equations are the steady-state forms of Faraday's law, Ampere's law, plus the steady-state forms of the relevant SRMHD equations:

Continuity:

$$\nabla \cdot (\gamma(v)\rho_0 \boldsymbol{v}) = 0, \tag{10}$$

Energy:

$$\nabla \cdot \left(\left[\gamma(v)^2(\mu + p) - \gamma(v)\rho_0 c^2 \right] \boldsymbol{v} + \frac{1}{\mu_0}(\boldsymbol{E} \times \boldsymbol{B}) \right) = 0. \tag{11}$$

Equation of State:

$$p = (\Gamma - 1)nu, \tag{12}$$

Isoentropicity:

$$\boldsymbol{v} \cdot \nabla \left(p/n^{\Gamma} \right) = 0, \tag{13}$$

Frozen-in-Flux:

$$\boldsymbol{E} + \boldsymbol{v} \times \boldsymbol{B} = 0, \tag{14}$$

Faraday:

$$\nabla \times \boldsymbol{E} = 0, \tag{15}$$

and Ampere:

$$\nabla \times \boldsymbol{B} = \mu_0 \boldsymbol{j}, \tag{16}$$

where $\boldsymbol{j}$ is the current density, p the pressure, Γ the adiabatic index, and c is the speed of light. Other quantities of interest are the Lorentz factor

$$\gamma(v) = \frac{1}{\sqrt{1 - \frac{v^2}{c^2}}}, \tag{17}$$

and μ is the proper energy density, where

$$\mu = nm_0c^2 + nu, \tag{18}$$

n is the rest frame particle number density, m_0 is the rest mass, nu is the rest frame, internal energy of the gas flow, $\rho_0 = m_0 n$, while $\boldsymbol{E}$ and $\boldsymbol{B}$ are the electric and magnetic fields in the laboratory frame.

Probably the most contentious of the above equations is the frozen-in-flux condition, equation (14). This equation is a consequence of a relatively simple, scalar form of Ohm's 'law' (see Appendix A). Ohm's law, typically, relates current flow to an applied electric field. In non-relativistic theory, a magnetic field embedded in a plasma gives rise to conductivities that allow the current to be decomposed into three separate currents, where one current flow is parallel to the magnetic field and the other two are perpendicular to the magnetic field. In many cases these latter 'Hall' and 'Pedersen' conductivities can be neglected, and the standard scalar form of Ohm's law (which gives rise to equation (14)) is obtained, but for a relativistic plasma it is not clear that such, and related, approximations are valid. For example, the mean velocities of the ions and electrons in a relativistic plasma may

https://doi.org/10.1071/AS01034 Published online by Cambridge University Press

be completely different. Such a phenomenon may lead to charge separation which in turn could produce a more complex form of Ohm's law and thereby make equation (14) invalid. In such a case, the single fluid model that is assumed in the above equations might have to be replaced with a model that describes the behaviour of the electrons and ions via separate equation systems.

For this paper, however, we use the simplest form of Ohm's law (and, as a consequence, equation (14)), because we are considering a relativistic flow condition that is not usually examined, i.e. where the direction of flow is perpendicular to the direction of the magnetic field. In Appendix A we discuss what constraints this approximation places on our solutions.

The frozen-in-flux condition, equation (14), forces the plasma to be tied to the magnetic field, so applying an $\boldsymbol{E}$ field perpendicular to $\boldsymbol{B}$ forces the charged particles and magnetic field to move in the $\boldsymbol{E} \times \boldsymbol{B}$ direction. To understand this behaviour, at a particulate level in the collisionless regime, we consider Figure 2. Here, positive particles rotate clockwise and negative particles rotate anticlockwise around a magnetic field $\boldsymbol{B}$ that is pointing out of the page. If we now subject the positive and negative particles to an electric field $\boldsymbol{E}$ then, initially, the positive particle moves in the same direction as the $\boldsymbol{E}$ field, while the negative particle moves in the opposite direction. The influence of the magnetic field, however, changes the path of both particles, so that they are moving in the same overall direction. The positive and negative particles, and the magnetic field, have the same velocity, i.e. the $\boldsymbol{E} \times \boldsymbol{B}$ velocity

$$\boldsymbol{v}_{E\times B} = \frac{\boldsymbol{E} \times \boldsymbol{B}}{B^2}. \tag{19}$$

It is of interest to compute the values of $\boldsymbol{E}$ and $\boldsymbol{B}$ in the co-moving reference frame, i.e. the frame of reference moving with the particles. Using the coordinate system of Figure 1, one can show (Ellis & Williams 1988) that

$$E'_{y'} = \gamma(v)\left(E_y - vB_z\right), \tag{20}$$

and

$$B'_{z'} = \gamma(v)\left(B_z - \frac{v}{c^2}E_y\right), \tag{21}$$

where the dashed quantities are measured in the co-moving reference frame, while the undashed quantities are in the 'stationary' laboratory frame. From equations (14) and (19), we see that

$$E_y = vB_z \tag{22}$$

which upon substitution into equations (20) and (21) gives

$$E'_{y'} = 0, \quad \text{and} \quad B'_{z'} = B_z/\gamma(v). \tag{23}$$

As expected, in the co-moving reference frame the electric field disappears, while the magnetic field is reduced by the factor $1/\gamma(v)$. In this frame, the particles gyrate around the magnetic field, with the radius of gyration increasing as the flow speed increases. A more detailed treatment of relativistic $\boldsymbol{E} \times \boldsymbol{B}$ drift is given in Appendix B.

Moving from the particulate to the continuum properties of the flow, we now derive the fundamental constants of the flow: (relativistic) mass, energy, magnetic flux, and entropy.

3.2 Constants of the Flow

The energy equation (equation (11)) has the information required to produce a flow solution. The Poynting vector term $\boldsymbol{E} \times \boldsymbol{B}$, in the energy equation, can be combined with the frozen-in-flux constraint (equation (14)) to give

$$\boldsymbol{E} \times \boldsymbol{B} = B^2\boldsymbol{v} - (\boldsymbol{v} \cdot \boldsymbol{B})\boldsymbol{B}. \tag{24}$$

Substituting equation (24) into the energy equation (equation (11)) gives

$$\nabla\cdot\left(\left(\gamma(v)^2(\mu + p) - \gamma(v)\rho_0c^2 + \frac{B^2}{\mu_0}\right)\boldsymbol{v} - \frac{(\boldsymbol{v}\cdot\boldsymbol{B})\boldsymbol{B}}{\mu_0}\right) = 0. \tag{25}$$

To obtain a constant of the flow, it is necessary to massage all the terms in equation (25) into the $\nabla\cdot(()\boldsymbol{v})$ term. This can only happen if $\boldsymbol{v} \perp \boldsymbol{B}$ or $\boldsymbol{v} \parallel \boldsymbol{B}$. The $\boldsymbol{v} \parallel \boldsymbol{B}$ case has been considered by other authors (e.g. Camenzind 1990) and will not be considered here. For $\boldsymbol{v} \perp \boldsymbol{B}$, equation (25) is simply

$$\nabla\cdot\left(\left(\gamma(v)^2(\mu + p) - \gamma(v)\rho_0c^2 + \frac{B^2}{\mu_0}\right)\boldsymbol{v}\right) = 0, \tag{26}$$

which has our desired conservative form.

Integrating equation (26) over the volume of the nozzle shown in Figure 1, and using Gauss' law gives

$$\begin{aligned}\int_V \nabla\cdot\left(\left(\gamma(v)^2(\mu + p) - \gamma(v)\rho_0c^2 + \frac{B^2}{\mu_0}\right)\boldsymbol{v}\right)dV \\ = \int_A \left(\gamma(v)^2(\mu + p) - \gamma(v)\rho_0c^2 + \frac{B^2}{\mu_0}\right)\boldsymbol{v}\cdot d\boldsymbol{A} \\ = 0,\end{aligned} \tag{27}$$

where V and A are the volume and cross-sectional surface aperture area of the nozzle, respectively. The flow cuts through the two end surfaces, so we can write

$$v_xA\left(\gamma(v)^2(\mu + p) - \gamma(v)\rho_0c^2 + \frac{B^2}{\mu_0}\right) = \text{constant}. \tag{28}$$

Similarly, from the continuity equation (equation (10)) we obtain the flow form of the mass conservation equation

$$v_xA\rho_0\gamma(v) = N_1, \tag{29}$$

where N_1 is a constant. Dividing equation (28) by equation (29) gives

$$\frac{\gamma(v)(\mu + p)}{\rho_0} - c^2 + \frac{B^2}{\gamma(v)\mu_0\rho_0} = \text{constant}. \tag{30}$$

Using equation (12), we can write

$$\mu + p = \rho_0c^2 + \frac{p\Gamma}{(\Gamma - 1)}. \tag{31}$$

https://doi.org/10.1071/AS01034 Published online by Cambridge University Press

Substituting equation (31) into equation (30) gives the relativistic MHD Bernoulli equation:

$$(\gamma(v)-1)c^2+\frac{\gamma(v)}{\Gamma-1}\frac{\Gamma p}{\rho_0}+\frac{1}{\gamma(v)}\frac{B^2}{\mu_0\rho_0}=N_2, \quad (32)$$

where N_2 is a constant.

We define the sound speed, C_S, by the equation

$$C_S^2=\frac{\gamma(v)\Gamma p}{\rho_0}, \quad (33)$$

and the Alfvén speed C_A by

$$C_A^2=\frac{B^2}{\gamma(v)\mu_0\rho_0}. \quad (34)$$

So we can rewrite the SRMHD Bernoulli equation (equation (32)) as

$$(\gamma(v)-1)c^2+\frac{1}{\Gamma-1}C_S^2+C_A^2=N_2. \quad (35)$$

To derive a constraint equation for the magnetic field, we combine the frozen-in-flux constraint with the Faraday law, equation (15), to obtain

$$\nabla\times(\boldsymbol{v}\times\boldsymbol{B})=0. \quad (36)$$

Integrating equation (36) over the cross section of the nozzle shown in Figure 3, and noting that the width, w (Figure 1), of the nozzle is kept constant, gives the equation for the conservation of the magnetic field in the flow:

$$v_x BA=N_3, \quad (37)$$

where N_3 is a constant.

Dividing the magnetic flow constant, equation (37), by the mass flow constant, equation (29), gives

$$\frac{B}{\rho_0\gamma(v)}=N_4. \quad (38)$$

So the magnitude of the magnetic field that helps drive the flow is directly proportional to the relativistic mass in the flow.

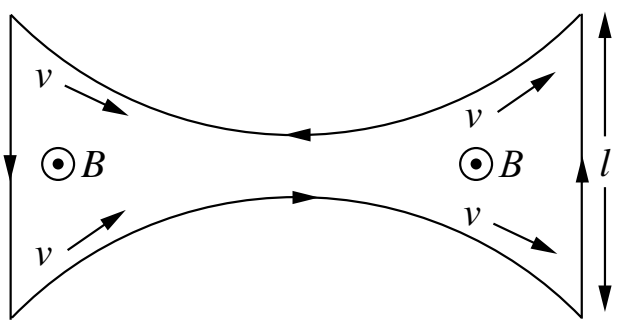

Figure 3 Cross section of the nozzle, showing the velocity of the flow, $\boldsymbol{v}$, and the direction of the magnetic field, $\boldsymbol{B}$. The arrows around the outer contour of the nozzle show the direction of integration of equation (36).

Finally we consider the steady-state form of the isoentropicity condition equation (13). This means, by definition, that p/n^Γ is a streamline constant of the flow, so

$$p=\kappa n^\Gamma \quad (39)$$

where κ is a constant. As discussed in Liffman (1998) for a collisionless, magnetically confined plasma, we should expect that $\Gamma=2$. If the plasma is not collisionless then $\Gamma<2$. In this paper, we will assume — unless stated otherwise — that $\Gamma=2$. For the case of $\Gamma<2$, the results of this paper are still applicable provided one assumes the cold plasma limit, $C_A\gg C_S$.

3.3 The Relativistic Nozzle Equation

To obtain the desired flow equation, we require a number of preliminary results. First, we take the differential of equation (17) to obtain

$$d(\gamma(v)-1)c^2=\gamma(v)^3 v\,dv. \quad (40)$$

Using equation (39) one can show

$$d\left(\frac{C_S^2}{\Gamma-1}\right)=\frac{C_S^2}{\Gamma-1}\left(\gamma(v)^2\frac{vdv}{c^2}+(\Gamma-1)\frac{dn}{n}\right). \quad (41)$$

Similarly, using equation (38), we have

$$d\left(C_A^2\right)=C_A^2\left(\gamma(v)^2\frac{vdv}{c^2}+\frac{dn}{n}\right). \quad (42)$$

So, the differential of the Bernoulli equation, equation (35), has the form

$$\gamma(v)^3v^2\frac{dv}{v}\left(1+\frac{C_S^2}{\gamma(v)(\Gamma-1)c^2}+\frac{C_A^2}{\gamma(v)c^2}\right)+\left(C_S^2+C_A^2\right)\frac{dn}{n}=0. \quad (43)$$

To massage equation (43) into our desired form, we use the mass flow constant equation (29) and equation (40) to obtain

$$\frac{dn}{n}=-\frac{dA}{A}-\frac{dv}{v}\left(1+\gamma(v)^2\frac{v^2}{c^2}\right), \quad (44)$$

where we have used the one-dimensional flow approximation $v_x\approx v$. Substituting equation (44) into equation (43) gives

$$\left(\frac{\gamma(v)^3v^2}{C_S^2+C_A^2}\left(1+\frac{C_S^2}{\gamma(v)c^2}\left(\frac{2-\Gamma}{\Gamma-1}\right)\right)-1\right)\frac{dv}{v}=\frac{dA}{A}. \quad (45)$$

Setting $\Gamma=2$ (or assuming that $\frac{C_S^2}{\gamma(v)c^2}\left(\frac{2-\Gamma}{\Gamma-1}\right)\ll 1$) gives the SRMHD nozzle equation

$$\left(\gamma(v)^3\frac{v^2}{C_S^2+C_A^2}-1\right)\frac{dv}{v}=\frac{dA}{A}. \quad (46)$$

To further understand the behaviour of equation (46), it is convenient to rewrite it in a more amenable form.

https://doi.org/10.1071/AS01034 Published online by Cambridge University Press

3.4 Normalised Form

At the start of the flow, described by equation (46), $v \approx 0$ and for dv to be greater than 0, we require $dA < 0$, i.e. the nozzle has to converge. The nozzle will reach its narrowest point, the so-called throat of the nozzle, when $dA = 0$. This occurs when

$$\frac{\gamma_T^3 v_T^2}{C_{ST}^2 + C_{AT}^2} = 1, \tag{47}$$

where, v_T, γ_T, C_{ST}, and C_{AT} are the values of v, $\gamma(v)$, C_S, and C_A at the throat. Setting $\Gamma = 2$, the SRMHD Bernoulli equation (equation (35)) at the throat is

$$(\gamma_T - 1)c^2 + C_{ST}^2 + C_{AT}^2 = N_2. \tag{48}$$

Combining equations (47) and (48) gives

$$N_2 = (\gamma_T - 1)c^2 + \gamma_T^3 v_T^2. \tag{49}$$

Returning to the $\Gamma = 2$ SRMHD Bernoulli equation

$$(\gamma(v) - 1)c^2 + C_S^2 + C_A^2 = N_2, \tag{50}$$

we can combine the above two equations to replace the $C_S^2 + C_A^2$ in equation (46) to give

$$\left(\frac{\gamma(v)^3 v^2}{(\gamma_T - \gamma(v))c^2 + \gamma_T^3 v_T^2} - 1 \right) \frac{dv}{v} = \frac{dA}{A}, \tag{51}$$

which is a convenient form for the analysis of the flow. One can show that the non-relativistic form of equation (51) is simply

$$\left(\frac{2v^2}{3v_T^2 - v^2} - 1 \right) \frac{dv}{v} = \frac{dA}{A}, \tag{52}$$

which, from the equations in Section 2, is the expected result.

4 Behaviour of the Flow

4.1 Shape and Exit Speed

One can show that equation (51) has the analytic solution

$$\frac{A(v)}{A_T} = \frac{v_T}{v} \frac{v_T^2 \gamma_T^3}{(\gamma_T - \gamma(v))c^2 + v_T^2 \gamma_T^3}, \tag{53}$$

where A_T is the value of A at the throat of the nozzle. If we define $A^* = A/A_T$ and $v^* = v/v_T$ we can rewrite equation (53) as

$$v^* \left(1 + \frac{(\gamma_T - \gamma(v))c^2}{v_T^2 \gamma_T^3} \right) = \frac{1}{A^*}, \tag{54}$$

which has the non-relativistic limit (see also Liffman 1998; Schoenberg et al. 1991)

$$v^* \left(\frac{3}{2} - \frac{v^{*2}}{2} \right) = \frac{1}{A^*}. \tag{55}$$

The shape of the flow, as given by equation (53), for different throat speeds is shown in Figure 4. Here we plot the normalised aperture, A^*, against the flow speed v. So, for a flow with a throat speed, v_T, of $0.1c$, the flow starts with an infinitely large nozzle aperture, which decreases to $A^* = 1$ at the throat and diverges again when $v \approx \sqrt{3} \times 0.1c$, just as one would expect from equation (55). This behaviour changes, however, once we obtain throat speeds in excess of $0.2c$. For such flows, the divergent section of nozzle occurs over a relatively smaller part of the flow space, until, for highly relativistic flows, the divergent section of the nozzle nearly disappears.

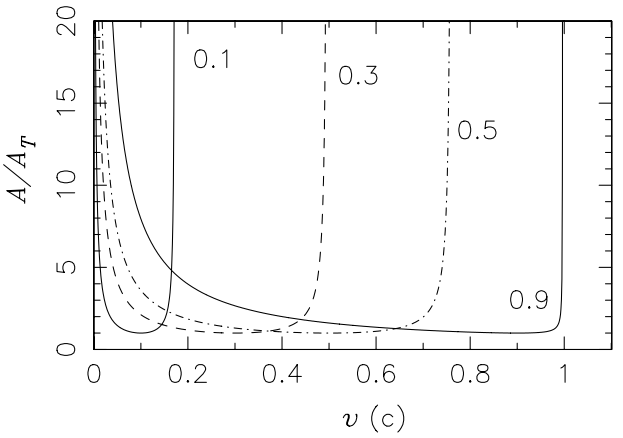

Figure 4 Nozzle shape as a function of flow speed. The numbers on each line give the flow speed at the throat of the nozzle. The velocity is in units of the speed of light. Non-relativistic flows have the standard convergent/divergent nozzle shape. Highly-relativistic flows also have a convergent/divergent shape, but the convergent section takes up nearly all of the flow space, the divergent section only occurring at the very end of the flow.

We can understand this behaviour by noting that, from equation (53), $A^*(0) = \infty$, $A^*(v_T) = 1$, and $A^*(v_E) = \infty$, where v_E is the exhaust speed of the nozzle, i.e. v_E is the root of the equation

$$(\gamma_T - \gamma(v))c^2 + v_T^2 \gamma_T^3 = 0, \tag{56}$$

which has the solution

$$v_E = c \sqrt{1 - \frac{c^4}{\gamma_T^2 \left(c^2 + v_T^2 \gamma_T^2 \right)^2}}. \tag{57}$$

In Figure 5 we plot the ratio $v_E/v_T \left(\equiv v_E^* \right)$ as a function of v_T, where v_T is in units of c. For $v_T \ll c$, $v_E^* = \sqrt{3}$, which is consistent with equation (55). Alternatively, when $v_T \to c$ then $v_E^* \to 1$, (i.e. $v_E \to c$), as one would expect.

4.2 Magnetic Field and Mass Density

From the mass and magnetic field conservation equations (equations (29) and (37), respectively), one can show that

$$\rho^* = B^*, \tag{58}$$

where $B^* = B/B_T$, B_T being the value of B at the throat of the nozzle, and ρ^* is the normalised mass density with $\rho^* = \rho/\rho_T$, where $\rho = \gamma(v)\rho_0$. In the rest of this section we will take the normalised magnetic field strength,

https://doi.org/10.1071/AS01034 Published online by Cambridge University Press

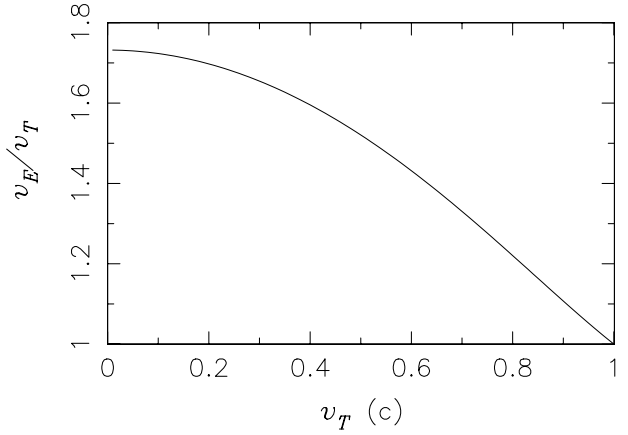

Figure 5 Normalised exit speed, v_E^*, as a function of the throat speed, v_T, where the throat speed is in units of c. Non-relativistic flows have $v_E = \sqrt{3}v_T$, while for highly-relativistic flows, $v_E \to c$.

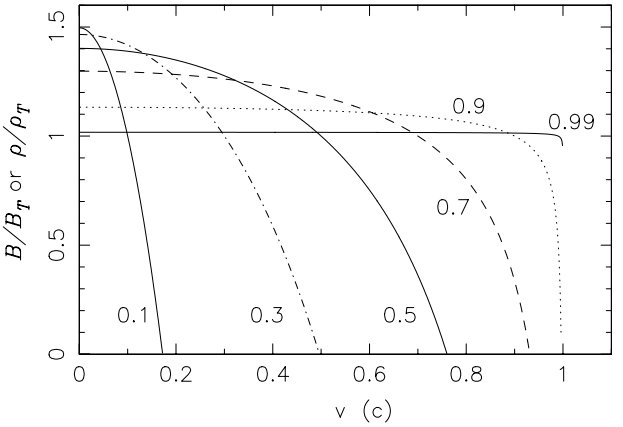

Figure 6 Normalised magnetic field strength, B^*, or gas mass density, ρ^*, as a function of flow speed of the nozzle, v, for different nozzles. Each line is labelled by the throat speed in units of c. For non-relativistic flows, B and $\rho \to 0$ as the flow leaves the nozzle. Highly relativistic flows, however, have B and $\rho \approx$ constant throughout the nozzle.

B^*, as being synonymous with the normalised mass density ρ^*.

Combining equations (37) and (54) gives an analytic solution for the normalised magnetic field strength

$$B^*(v) = 1 + \frac{(\gamma_T - \gamma(v))c^2}{v_T^2 \gamma_T^3}, \tag{59}$$

which implies that $B^*(v_T) = 1$, and that $B^*(0) \to 3/2$ for $v_T \ll c$. That is, for non-relativistic flows, the initial value of the magnetic field strength is 3/2 times its value at the throat of the nozzle. For highly relativistic flows, $B^*(0) \to 1$ when $v_T \to c$, so the magnetic field strength is nearly constant from the start through to the throat of the nozzle. For all cases, $B^*(v_E) = 0$, which implies that for a perfect nozzle, with an infinitely wide exit aperture area, the magnetic field strength at the exit is negligible relative to its value at the start of the flow. If a nozzle is less than perfect, however, then the exit aperture will have finite area and non-relativistic nozzles will produce a jet with a relatively small magnetic field, while relativistic jets may have magnetic fields comparable to those at the start of the flow.

The behaviour of the normalised magnetic field as a function of the jet flow speed is shown in Figure 6. The non-relativistic case is shown by the line labelled with 0.1. This line represents the value of ρ^* and B^* for a flow with a throat speed of $0.1c$. At the start of the flow $v = 0$, and $B^* = 1.5$. When $v = 0.1$ the flow has reached the throat of the nozzle and $B^* = 1.0$. Finally when $v = 0.1 \times \sqrt{3}$, the flow is at the exit of the nozzle and, as expected, $B^* = 0.0$. For the highly relativistic case, we have the line labelled 0.99. This line shows the behaviour of the flow for a nozzle with a throat speed of $0.99c$. For this flow, $B^* \approx 1$ throughout the nozzle, except for when the flow speed $\approx c$, a remarkable contrast in behaviour relative to the non-relativistic case. The remaining lines show the intermediate behaviour of the flow between the non and highly relativistic flows.

The magnitude of B decreases as the flow travels through the nozzle, because the magnetic pressure ($= B^2/2\mu_0$) has to decrease along the nozzle, to drive the flow. Quantitatively, one can see this by taking the differentials of equations (29) and (38):

$$\frac{d\rho_0}{\rho_0} + \frac{dv}{v} + \frac{d\gamma(v)}{\gamma(v)} + \frac{dA}{A} = 0, \tag{60}$$

and

$$\frac{dB}{B} = \frac{d\rho_0}{\rho_0} + \frac{d\gamma(v)}{\gamma(v)}. \tag{61}$$

Combining the above equations gives

$$\frac{dB}{B} + \frac{dv}{v} + \frac{dA}{A} = 0, \tag{62}$$

which in turn can be combined with equation (46) to show the relative variation of B as a function of the relative variation in v

$$\frac{dB}{B} = -\frac{\gamma(v)^3 v^2}{C_F^2}\frac{dv}{v}, \tag{63}$$

so for increasing v (i.e. $dv > 0$), B must decrease, although highly relativistic flows ($C_F \gtrsim c$) will have a smaller decrease in B.

This near constancy in B, for highly relativistic jets, may have some intriguing consequences for astronomy, since many relativistic jets observed in nature appear to have 'radio-loud' and 'radio-quiet' phases. This behaviour has been interpreted as showing the presence/absence of a magnetic field within the jet flow. There is no generally accepted explanation for this behaviour. In our model, however, such behaviour appears to be a natural consequence of the flow equations.

4.3 Speed, Energetics and Length Scale

By convention, the start of the nozzle is called the 'reservoir'. The speed of the flow at this point, v_R, is zero.

https://doi.org/10.1071/AS01034 Published online by Cambridge University Press

So the Bernoulli equation is

$$C_{SR}^2 + C_{AR}^2 = C_{FR}^2 = N_2, \tag{64}$$

where C_{SR}, C_{AR} and C_{FR} are the sound, Alfvén and fast magnetosonic speeds at the reservoir, respectively.

Combining equations (64) and (49) gives

$$(\gamma_T - 1)c^2 + \gamma_T^3 v_T^2 = C_{FR}^2, \tag{65}$$

which, from equation (57), gives an exit speed of

$$v_E = c\sqrt{1 - \frac{c^4}{\left(C_{FR}^2 + c^2\right)^2}}. \tag{66}$$

In the non-relativistic limit ($c \gg C_{FR}$), equation (66) implies that $v_E = \sqrt{2}C_{FR}$, while in the relativistic limit ($C_{FR} \gg c$)

$$v_E \approx c\sqrt{1 - (c/C_{FR})^4} \approx c. \tag{67}$$

Thus, the exit speed for a non-relativistic jet is proportional to the fast magnetosonic speed at the reservoir, but this proportionality disappears as C_{FR} becomes relativistic.

The kinetic energy of a particle that is ejected by the nozzle, E_K, takes the form

$$E_K = m_0(\gamma(v_E) - 1)c^2 = m_0 C_{FR}^2, \tag{68}$$

where m_0 is the rest mass of the particle. Equation (68) is a general result that is true for both relativistic and non-relativistic flow. For a proton, $m_0c^2 \approx 938\,\text{MeV}$, and so to obtain (say) a 1 TeV proton (or a 556 MeV electron) we require $C_{FR} \approx 33c$. We can control the speed and energy of the flow by changing the Alfvén speed at the reservoir, which means we change the reservoir magnetic field strength, B_R, and/or the reservoir mass density, ρ_R, since $C_{AR} = B_R/\sqrt{\mu_0\rho_R}$, where μ_0 is the permeability of free space. For fully ionised hydrogen, C_{AR} has the parameterisation

$$C_{AR} = 32.5c\left(\frac{B_R}{10\,\text{T}}\right)\left(\frac{n_R}{10^{15}\,\text{m}^{-3}}\right)^{-1/2}, \tag{69}$$

where n_R is the number density of the hydrogen plasma at the reservoir. That is, for a number density of $10^{15}\,\text{m}^{-3}$, we require $B_R \approx 10$ tesla to obtain $C_{AR} \approx 33c$.

In principle, we should be able to construct a relativistic jet that produces particles of arbitrary high energies simply by setting the appropriate Alfvén speed for the jet flow. In practice, however, it is unlikely that a laboratory scale TeV device can be built with current technology, although a galactic or stellar version of this type of jet may be feasible. To see why this is so, we now consider the minimum length scale for this system.

From Appendix B the relativistic gyroradius is

$$r_g = \frac{m_0\gamma^2 E}{qB^2}, \tag{70}$$

which has the parameterised form

$$r_g = 3.127\,\gamma^2\frac{(m_0/m_p)(f/1)}{(q/e)(B/1\,\text{T})}\,\text{m}, \tag{71}$$

where m_p is the rest mass of the proton, e is the electric charge of an electron, and f is the $E \times B$ drift speed as a fraction of c, i.e. $v_{\text{drift}} = E/B = fc$. Assuming $B = 1\,\text{T}$, a TeV proton would give $f \approx 1$, $\gamma = 1067$, and, from equation (71), $r_g = 3560\,\text{km}$. To build a TeV nozzle the width at the throat of the nozzle would have to be at least $2r_g$, which is larger than the radius of the Earth. This is beyond current engineering capability, but it is small relative to expected formation length scales of astrophysical jets.

We can also obtain an estimate on the lower limit of the allowed gas density, because in our derivation of the SRMHD nozzle equation (equation (46)), we ignored the displacement current (cf. equations (16) and (115)). This is equivalent to assuming that $\nabla\cdot\boldsymbol{j} = 0$ (equation (16)), i.e. there is no source term for the current or no accumulation of charge. More carefully one can show

$$\nabla\cdot\boldsymbol{j} \sim O\left(\left(V^2/c^2\right)B/\mu_0 L^2\right), \tag{72}$$

where V is a characteristic speed of the system and L a suitable length scale.

After some manipulation, one can turn equation (72) into a condition for the gas to remain electrically neutral:

$$n \gg \frac{\epsilon_0 VB}{eL} \approx 1.10\times 10^6\,\frac{(V/c)(B/1\,\text{T})}{(L/0.1\,\text{AU})}\,\text{m}^{-3}, \tag{73}$$

where e is the electric charge and ϵ_0 the permittivity of free space. It is probable that most astrophysical sources would satisfy equation (73).

5 Conclusions

In this paper, we have derived the special relativistic magnetohydrodynamic equations and used these equations to find analytic solutions for a one-dimensional, relativistic, magnetically driven jet flow. We have shown that magnetic field gradients can accelerate a plasma to highly relativistic speeds. We have also shown that the kinetic energy, E_K, of a particle that is leaving the nozzle is given by the equation $E_K = m_0 C_{FR}^2$, where m_0 is the rest mass of the particle and C_{FR} is the fast magnetosonic speed at the start of the flow.

A relativistic MHD nozzle differs in a number of ways from the standard, non-relativistic MHD nozzle. A non-relativistic nozzle has a converging/diverging shape, while a highly relativistic nozzle converges in the usual manner, but diverges in an abrupt fashion only at the very end of the nozzle. The gentle divergence of non-relativistic nozzles causes the exit plasma densities and magnetic fields of the flow to have values that are small relative to their values at the start of the nozzle. The abrupt divergence of relativistic nozzles implies that a less than perfect nozzle will produce a jet with a magnetic field strength comparable to the initial driving field.

https://doi.org/10.1071/AS01034 Published online by Cambridge University Press

This behaviour may have an astrophysical counterpart. For example, relativistic jets are observed from the centres of galaxies, and even from compact stellar systems in our own Galaxy (Mirabel & Rodriguez 1998). Such jets appear to have two states sometimes known as 'radio-loud' and 'radio-quiet'. This behaviour has been interpreted as showing the presence/absence of a magnetic field within the jet flow. Currently, there is some uncertainty in understanding why relativistic jets show this behaviour. In our jet model, such behaviour would appear to be a natural consequence of the flow equations. Simply put, high energy, relativistic flows will probably contain magnetic fields that are of similar magnitude to the driving source fields. On the other hand, low energy, low speed flows will very probably contain magnetic fields that are much smaller in magnitude than the driving source fields. Our model indicates that there is no sharp dividing line between these two states. Instead there would appear to be a continuum of jet flows of which the 'radio-loud' and 'radio-quiet' flows are the extreme endpoints.

It will take a more detailed model to determine whether the observed relativistic jets are driven by the MHD mechanism outlined in this study, but this work raises the tantalising possibility that we may have uncovered Nature's own plasma accelerator.

A The Special Relativistic MHD Equations

To obtain the SRMHD equations, we consider a stress energy tensor that is made of two separate parts:

$$T^{\alpha\beta} = T^{\alpha\beta}_{\text{part}} + T^{\alpha\beta}_{\text{em}} \tag{74}$$

where $T^{\alpha\beta}$ is the total stress energy tensor, $T^{\alpha\beta}_{\text{part}}$ is the 'particle' stress energy tensor and $T^{\alpha\beta}_{\text{em}}$ is the electromagnetic stress energy tensor.

The particle stress energy tensor describes a perfect, inviscid fluid and has the form (Landau & Lifshitz 1997; Weinberg 1972)

$$T^{\alpha\beta}_{\text{part}} = (\mu + p)U^{\alpha}U^{\beta} + pg^{\alpha\beta}, \tag{75}$$

where μ is the proper energy density, i.e.

$$\mu = nm_0c^2 + nu, \tag{76}$$

n being the rest frame particle number density, m_0 is the rest mass, and nu is the rest frame, internal energy of the gas flow, p is the pressure, U^{α} is the four-velocity, i.e.

$$(U^{\alpha}) = \gamma(v)(1, \boldsymbol{v}/c), \tag{77}$$

and $g^{\alpha\beta}$ is the metric tensor, which, for this paper, has the form

$$g^{\alpha\beta} = \begin{pmatrix} -1 & 0 & 0 & 0 \\ 0 & 1 & 0 & 0 \\ 0 & 0 & 1 & 0 \\ 0 & 0 & 0 & 1 \end{pmatrix}. \tag{78}$$

It can be shown that

$$T^{00}_{\text{part}} = \gamma(v)^2\left(\mu + \frac{pv^2}{c^2}\right), \tag{79}$$

$$T^{0i}_{\text{part}} = T^{i0}_{\text{part}} = \gamma(v)^2(\mu + p)\frac{v^i}{c}, \tag{80}$$

and

$$T^{ij}_{\text{part}} = T^{ji}_{\text{part}} = \gamma(v)^2(\mu + p)\frac{v^iv^j}{c^2} + p\delta^{ij}, \tag{81}$$

where δ^{ij} is the Kronecker delta function.

The stress-energy tensor for the electromagnetic field is given by (Ellis & Williams 1988)

$$T^{\alpha\beta}_{\text{em}} = \epsilon_0\left(F^{\alpha}_{\gamma}F^{\beta\gamma} - \frac{1}{4}g^{\alpha\beta}F^{\gamma\delta}F_{\gamma\delta}\right), \tag{82}$$

where ϵ_0 is the permittivity of free space, $F^{\alpha\beta}$ is the electromagnetic field tensor which is given by

$$F^{\alpha\beta} = c\begin{pmatrix} 0 & E_x/c & E_y/c & E_z/c \\ -E_x/c & 0 & B_z & -B_y \\ -E_y/c & -B_z & 0 & B_x \\ -E_z/c & B_y & -B_x & 0 \end{pmatrix}, \tag{83}$$

where $\boldsymbol{E} = (E_x, E_y, E_z)$ is the electric field and $\boldsymbol{B} = (B_x, B_y, B_z)$ is the magnetic field, where both $\boldsymbol{E}$ and $\boldsymbol{B}$ are measured in the laboratory frame.

The electromagnetic field tensor allows us to write the four dimensional form of Maxwell's equation in flat space–time:

$$\frac{\partial F_{\alpha\beta}}{\partial x^{\gamma}} + \frac{\partial F_{\gamma\alpha}}{\partial x^{\beta}} + \frac{\partial F_{\beta\gamma}}{\partial x^{\alpha}} = 0, \tag{84}$$

and

$$\frac{1}{c}\frac{\partial F^{\alpha\beta}}{\partial x^{\beta}} = \frac{1}{\epsilon_0}J^{\alpha}, \tag{85}$$

where J^{α} is the current four-vector and has the definition

$$(J^{\alpha}) = \gamma(v)\rho_{c0}(1, \boldsymbol{v}/c), \tag{86}$$

ρ_{c0} being the rest charge density.

Combining equations (82), (84), and (85) with some indicial gymnastics gives

$$\frac{\partial T^{\mu\nu}_{\text{em}}}{\partial x^{\nu}} = T^{\mu\nu}_{\text{em},\nu} = -cF^{\mu\alpha}J_{\alpha}. \tag{87}$$

After some computation, one can show

$$T^{00}_{\text{em}} = \frac{1}{2}\epsilon_0\left(E^2 + c^2B^2\right), \tag{88}$$

$$T^{ij}_{\text{em}} = \epsilon_0\left\{\left(E^2 + c^2B^2\right)g^{ij} - E^iE^j - c^2B^iB^j\right\}, \tag{89}$$

and

$$T^{0i}_{\text{em}} = T^{i0}_{\text{em}} = \frac{1}{c\mu_0}(\boldsymbol{E} \times \boldsymbol{B})^i, \tag{90}$$

where μ_0 is the permeability of free space and ϵ_0, μ_0 satisfy the equation

$$\epsilon_0\mu_0 = 1/c^2. \tag{91}$$

From Battaner (1996), we have

$$T^{\alpha\beta}_{,\beta} = T^{\alpha\beta}_{\text{part},\beta} + T^{\alpha\beta}_{\text{em},\beta} = 0. \tag{92}$$

https://doi.org/10.1071/AS01034 Published online by Cambridge University Press

If we unwrap equation (92), we find

$$T^{\alpha\beta}_{\ ,\beta} = \frac{\partial\left((\mu+p)U^\alpha U^0\right)}{\partial t} + \frac{\partial\left((\mu+p)U^\alpha U^j\right)}{\partial(x^j/c)} + \frac{\partial\left(pg^{\alpha 0}\right)}{\partial t} + \frac{\partial\left(pg^{\alpha j}\right)}{\partial(x^j/c)} + \epsilon_0\frac{\partial\left(F^\alpha_\gamma F^{0\gamma}\right)}{\partial t} + \epsilon_0\frac{\partial\left(F^\alpha_\gamma F^{j\gamma}\right)}{\partial\left(x^j/c\right)} - \frac{\epsilon_0}{4}g^{\alpha 0}\frac{\partial\left(F^{\gamma\delta}F_{\gamma\delta}\right)}{\partial t} - \frac{\epsilon_0}{4}g^{\alpha j}\frac{\partial\left(F^{\gamma\delta}F_{\gamma\delta}\right)}{\partial(x^j/c)} = 0, \quad (93)$$

where we have set

$$(x^\alpha) = (t, \boldsymbol{x}/c), \quad (94)$$

and we now have the machinery to derive the relativistic MHD equations.

Conservation of Rest Mass Density

Conservation of rest mass density follows directly from the conservation of particle number. The standard definition for the number flux four-vector is

$$N^\alpha = nU^\alpha. \quad (95)$$

The rate of change of the number of particles in a fluid element will be due only to loss or gain of particles across the boundaries of the fluid element, which implies

$$N^\alpha_{\ ,\alpha} = 0, \quad (96)$$

which is the relativistic continuity equation

$$\frac{\partial(\gamma(v)\rho_0)}{\partial t} + \nabla\cdot(\gamma(v)\rho_0\boldsymbol{v}) = 0, \quad (97)$$

where $\rho_0 = m_0 n$.

Conservation of Momentum

If we set $\alpha = i$ in equation (93), we obtain the relativistic momentum conservation equation

$$\frac{\partial(\gamma(v)^2(\mu+p)\boldsymbol{v}/c^2 + \epsilon_0(\boldsymbol{E}\times\boldsymbol{B}))}{\partial t} + \nabla\cdot\left(\gamma(v)^2\frac{(\mu+p)}{c^2}\boldsymbol{v}\boldsymbol{v} + p\mathbf{I} - \mathbf{M}\right) = 0, \quad (98)$$

where $\mathbf{I}$ is the identity tensor (i.e. δ^{ij}), and $\mathbf{M}$ is the Maxwell stress tensor, which has the form

$$\mathbf{M} = \epsilon_0\boldsymbol{E}\boldsymbol{E} + \frac{\boldsymbol{B}\boldsymbol{B}}{\mu_0} - \left(\frac{B^2}{2\mu_0} + \epsilon_0\frac{E^2}{2}\right)\mathbf{I}. \quad (99)$$

There are two sections of equation (98) which are easily recognisable. First there is the relativistic hydrodynamic momentum equation (e.g. Chow & Monaghan 1997)

$$\frac{\partial(\gamma(v)^2(\mu+p)\boldsymbol{v}/c^2)}{\partial t} + \nabla\cdot\left(\gamma(v)^2\frac{(\mu+p)}{c^2}\boldsymbol{v}\boldsymbol{v} + p\mathbf{I}\right) = 0, \quad (100)$$

and one can show — after some considerable manipulation — that the remaining electromagnetic terms are simply the Lorentz force density

$$\nabla\cdot\mathbf{M} - \frac{\partial(\epsilon_0(\boldsymbol{E}\times\boldsymbol{B}))}{\partial\mathbf{t}} = \rho_c\boldsymbol{E} + \boldsymbol{j}\times\boldsymbol{B}, \quad (101)$$

where ρ_c is the charge density.

So, equation (98) has the expected force structure, and one can show that the non-relativistic limit of equation (98) is the standard MHD momentum equation.

Conservation of Energy

If we set $\alpha = 0$ in equation (93), we obtain

$$\frac{\partial\left(\gamma(v)^2(\mu+p) - p + \frac{B^2}{2\mu_0} + \epsilon_0\frac{E^2}{2}\right)}{\partial t} + \nabla\cdot\left(\gamma(v)^2(\mu+p)\boldsymbol{v} + \frac{1}{\mu_0}(\boldsymbol{E}\times\boldsymbol{B})\right) = 0. \quad (102)$$

Equation (102) is an energy equation, but it does not have the desired non-relativistic limit, since it includes the energy associated with the rest mass. We take the view that the rest mass energy has little or no relevance to the kinematics of the flow, so we multiply equation (97) by c^2 and subtract the result from equation (102) to obtain the relativistic MHD energy equation

$$\frac{\partial\left(\gamma(v)^2(\mu+p) - p - \gamma(v)\rho_0c^2 + \frac{B^2}{2\mu_0} + \epsilon_0\frac{E^2}{2}\right)}{\partial t} + \nabla\cdot\left(\left[\gamma(v)^2(\mu+p) - \gamma(v)\rho_0c^2\right]\boldsymbol{v} + \frac{1}{\mu_0}(\boldsymbol{E}\times\boldsymbol{B})\right) = 0. \quad (103)$$

The hydrodynamic part of equation (103)

$$\frac{\partial\left(\gamma(v)^2(\mu+p) - p - \gamma(v)\rho_0c^2\right)}{\partial t} + \nabla\cdot\left(\left[\gamma(v)^2(\mu+p) - \gamma(v)\rho_0c^2\right]\boldsymbol{v}\right) \quad (104)$$

has been developed and used by other authors (Martí 1996). The electromagnetic terms

$$\frac{\partial\left(\frac{B^2}{2\mu_0} + \epsilon_0\frac{E^2}{2}\right)}{\partial t} + \nabla\cdot\left(\frac{1}{\mu_0}(\boldsymbol{E}\times\boldsymbol{B})\right) = -\boldsymbol{j}\cdot\boldsymbol{E} \quad (105)$$

are the standard equations that occur in the regular MHD energy equation. For our purposes, the most important term in equation (105) is the Poynting flux $(1/\mu_0(\boldsymbol{E}\times\boldsymbol{B}))$. As we discuss in Section 3.2, if we wish to conserve energy along a jet flow, the Poynting flux constrains the flow to be either parallel or perpendicular to the magnetic field.

Equation of State

For our equation of state, we choose the ideal gas equation (Weinberg 1972)

$$p = (\Gamma - 1)nu, \quad (106)$$

where Γ is the adiabatic index.

https://doi.org/10.1071/AS01034 Published online by Cambridge University Press

Isoentropicity

The adiabatic/isoentropic condition implies (Weinberg 1972) that

$$\frac{\partial\left(p/n^{\Gamma}\right)}{\partial t}+\boldsymbol{v}\cdot\nabla\left(p/n^{\Gamma}\right)=0. \tag{107}$$

Frozen-in-Flux, Ohm's Law

If we assume that the rest frame density of the electric charge is zero, then, for the simplest case, the current four-vector J^{α} is given by Ohm's law:

$$J^{\alpha}=\sigma F^{\alpha\beta}U_{\beta}, \tag{108}$$

where σ is the conductivity. So, an infinitely conducting medium (i.e. $\sigma=\infty$) requires that

$$F^{\alpha\beta}U_{\beta}=0. \tag{109}$$

If one solves the temporal and spatial parts of equation (109) we obtain, respectively

$$\boldsymbol{E}\cdot\boldsymbol{v}=0 \tag{110}$$

and

$$\boldsymbol{E}+\boldsymbol{v}\times\boldsymbol{B}=0. \tag{111}$$

Equation (111) implies equation (110) and so equation (111) is our (and the standard) frozen-in-flux condition. However, as discussed in Section 2, there is some uncertainty as to how appropriate is the use of equations (108) and (111) in relativistic MHD. This and related questions have been discussed by a number of authors, e.g. Ardavan (1976), Blackman & Field (1993), Melatos & Melrose (1996), and Khanna (1998). A thorough review of the results these, and other, authors have obtained is beyond the scope of this paper. Instead we shall list some of the general results that may constrain the use of equation (111).

Firstly, if we assume an approximately neutral plasma, i.e. $Zn_i\approx n_e$ (where Z is the charge on the main ion under consideration, while n_i and n_e are the rest frame number density of the ions and the electrons, respectively), then we obtain the constraint $\gamma(v_i)\approx\gamma(v_e)$, where v_i, and v_e are the 'bulk' speeds of the ions and electrons. In addition, in order to describe the plasma as a single fluid the constraints increase and we have $\gamma(v_i)\approx\gamma(v_e)\approx\gamma(v)$ plus we also require $p\ll nm_0c^2$, and $nu\ll nm_0c^2$, i.e. the specific internal energy of the gas and the pressure have to be small relative to the rest mass energy density. With such constraints, it is possible to show that for this 'cold', neutral plasma, the relativistic form of Ohm's law reduces to the standard non-relativistic form of Ohm's law. The simple, scalar form of Ohm's law, and the associated frozen-in-flux condition equation (111), is then obtained in the standard manner by ensuring that the cyclotron frequencies of the electrons and ions and the associated collision frequencies (plus the electron pressure gradient) have the appropriate values such that the Hall, Pedersen and associated conductivities can be neglected.

Maxwell's Equations

Finally, to solve for $\boldsymbol{E}$ and $\boldsymbol{B}$, we need Maxwell's equations:

Gauss:

$$\nabla\cdot\boldsymbol{E}=\rho_c/\epsilon_0, \tag{112}$$

Gilbert:

$$\nabla\cdot\boldsymbol{B}=0, \tag{113}$$

Faraday:

$$\nabla\times\boldsymbol{E}=-\frac{\partial B}{\partial t}, \tag{114}$$

and Ampere:

$$\nabla\times\boldsymbol{B}=\mu_0\boldsymbol{j}+\mu_0\epsilon_0\frac{\partial E}{\partial t}. \tag{115}$$

B Length and Time Scales of Relativistic $\boldsymbol{E}\times\boldsymbol{B}$ Drift

Unfortunately the derivation of the relativistic nozzle equation (Section 3) does not provide the fundamental length and time scales to describe the flow. To obtain a set of such length scales, we examine the relativistic $\boldsymbol{E}\times\boldsymbol{B}$ drift, since this is probably the main physical mechanism that allows charged particles to move through a magnetic nozzle.

Using Minkowski coordinates in flat space–time, the motion of a charged particle under electromagnetic forces is determined by the force law

$$\frac{dP^{\alpha}}{d\tau}=\left(\frac{q}{c}\right)F^{ab}U_b, \tag{116}$$

where τ is the proper time, q is the charge of the particle, and $\boldsymbol{P}$ is the four-momentum, i.e.

$$(P^{\alpha})=m_0(U^{\alpha})=m_0\gamma(v)(1,\boldsymbol{v}/c). \tag{117}$$

If we unwrap equation (116), we obtain two separate equations that describe the motion of a relativistic, charged particle (Ellis & Williams 1988):

$$\frac{d\left(\gamma m_0\boldsymbol{v}\right)}{dt}=q(\boldsymbol{E}+\boldsymbol{v}\times\boldsymbol{B}), \tag{118}$$

and

$$\frac{d\left(\gamma m_0c^2\right)}{dt}=q\boldsymbol{E}\cdot\boldsymbol{v}. \tag{119}$$

For the case where, in cartesian coordinates, $\boldsymbol{E}=(0,E,0)$ and $\boldsymbol{B}=(0,0,B)$, equation (119) becomes

$$\frac{d\gamma}{dt}=\frac{qEv_y}{m_0c^2}. \tag{120}$$

Combining equations (120) and (118) gives

$$\frac{dv_x}{dt}=\frac{q}{m_0\gamma}\left[v_yB-\frac{Ev_xv_y}{c^2}\right], \tag{121}$$

https://doi.org/10.1071/AS01034 Published online by Cambridge University Press

$$\frac{dv_y}{dt} = \frac{q}{m_0\gamma}\left[E\left(1-\left(\frac{v_y}{c}\right)^2\right) - v_x B\right], \qquad (122)$$

and

$$\frac{dv_z}{dt} = \frac{qEv_z v_y}{m_0\gamma c^2}. \qquad (123)$$

We will assume $v_z(0) = 0$, in which case equation (123) implies that $v_z(t) = 0\ \forall\ t$, and the particle motion is confined to the x–y plane.

To improve our understanding of relativistic $\boldsymbol{E} \times \boldsymbol{B}$ drift it is instructive to first consider the *non-relativistic case*.

Suppose that $|\boldsymbol{v}| \ll c$, then equations (121) and (122) become

$$\frac{dv_x}{dt} = \frac{qB}{m_0}v_y, \qquad (124)$$

and

$$\frac{dv_y}{dt} = \frac{q}{m_0}E - \frac{qB}{m_0}v_x. \qquad (125)$$

which have the solutions (for the initial conditions $\boldsymbol{v}(0) = 0$)

$$v_x = \frac{E}{B}(1-\cos\omega t), \qquad (126)$$

and

$$v_y = \frac{E}{B}\sin\omega t, \qquad (127)$$

where $\omega = qB/m_0$ is the non-relativistic, angular cyclotron frequency. Equations (126) and (127) indicate that the charged particle moves in a circular fashion around a guiding centre, where the rotation speed of the particle around its guiding centre is equal to the translation speed (E/B) of the guiding centre. Equations (126) and (127) can be integrated to show that the radius of gyration or gyroradius, r_g, is given by the equation

$$r_g = \left|\frac{mE}{qB^2}\right|. \qquad (128)$$

For the *relativistic case*, where $|\boldsymbol{v}|$ is a significant fraction of c, there appears to be no general, analytic solution of equations (121) and (122). However, if we set $\boldsymbol{E} = \boldsymbol{0}$ then equation (119) implies that γ is a constant and equations (121) and (122) become

$$\frac{dv_x}{dt} = \omega v_y, \qquad (129)$$

and

$$\frac{dv_y}{dt} = -\omega v_x, \qquad (130)$$

where now ω is the relativistic gyrofrequency,

$$\omega = \frac{qB}{m_0\gamma}. \qquad (131)$$

Thus we have relativistic circular motion around a magnetic field line with a gyroradius, r_g, given by the equation

$$r_g = \frac{m_0\gamma}{qB}\sqrt{v_{x0}^2 + v_{y0}^2}, \qquad (132)$$

where v_{x0} and v_{y0} are the initial values for the x and y components of the particle's speed. As discussed in Section 3.1, a particle undergoing $\boldsymbol{E}\times\boldsymbol{B}$ drift sees no electric field in the comoving frame. Hence, we can assume that our particle is undergoing $\boldsymbol{E} \times \boldsymbol{B}$ drift in the $\boldsymbol{x}$ direction. As a consequence of equations (126) and (127) one has $\sqrt{v_{x0}'^2 + v_{y0}'^2} = E/B$, where v_{x0}' and v_{y0}' are the initial velocity components in the comoving frame plus E and B are now the electric and magnetic field strengths in the 'stationary' laboratory frame. Also, from equation (23), $B' = B/\gamma$, where B' is the magnetic field strength in the comoving frame. Putting this information together gives

$$r_g = \frac{m_0\gamma}{qB'}\sqrt{v_{x0}'^2 + v_{y0}'^2} = \frac{m_0\gamma^2 E}{qB^2}, \qquad (133)$$

where we note that

$$\gamma = \frac{cB}{\sqrt{c^2B^2 - E^2}}, \qquad (134)$$

with $E < cB$. Since the motion of the particle is in the $\boldsymbol{x}$ direction, then $2r_g$ gives the width of the particle motion in the $\boldsymbol{y}$ direction. To check on this, we can obtain an independent value for r_g by solving equations (121), and (122) with the NDSolve utility in Mathematica 3.0. This code uses five different numerical methods to solve a given system of differential equations (Wolfram 1996). The results of these calculations for the motion of a proton are shown in Figure 7, where we plot r_g (in units of metres) versus γ. The unbroken lines give the analytic results from equations (133) and (134), where the numbers on each line give the assumed magnetic field strength in units of teslas. The points on each line are obtained from the numerical integration of equations (121), and (122). Due to numerical difficulties we could not plot beyond $E/B = 0.999c$ or $\gamma \approx 22.3$. As can be seen, there is good agreement between the analytic and numerical solutions.

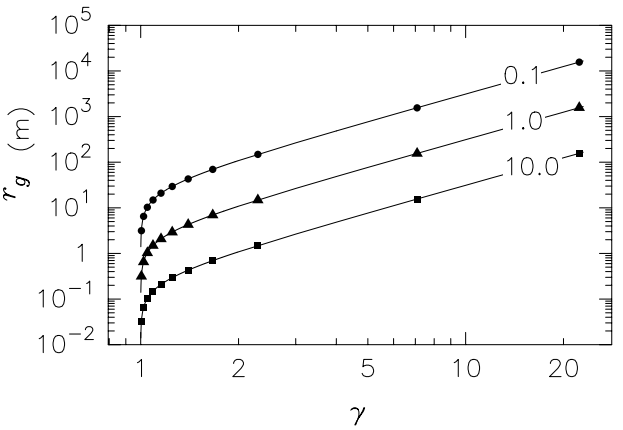

Figure 7 Relativistic gyroradius, r_g, versus γ. The points represent values from the numerical solution of equations (121) and (122), while the lines are obtained from the analytic solution (equations (133) and (134)). The numbers on the lines show the assumed values of B in units of teslas.

https://doi.org/10.1071/AS01034 Published online by Cambridge University Press

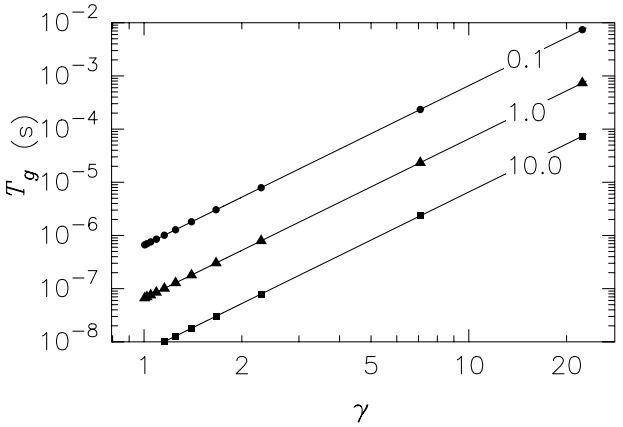

Figure 8 Relativistic gyration period, T_g, versus γ. The points represent values from the numerical solution of equations (121) and (122), while the lines are obtained from the analytic solution (equation (135)). The numbers on the lines show the assumed values of B in units of teslas.

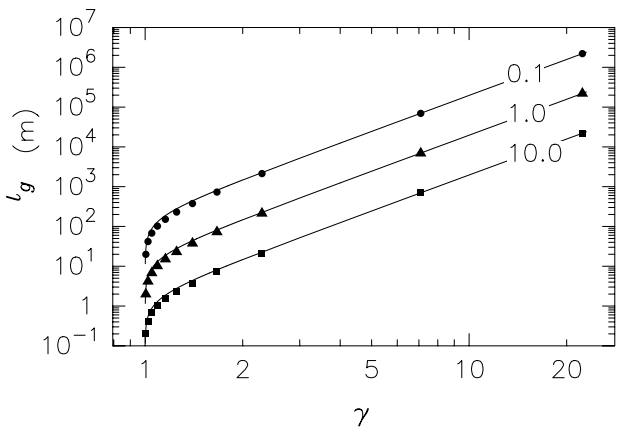

Figure 9 Length of gyration, l_g, versus γ. The points represent values from the numerical solution of equations (121) and (122), while the lines are obtained from the analytic solution (equation (138)). The numbers on the lines show the assumed values of B in units of teslas.

Equation (133) provides us with a length scale for determining the width of the nozzle, since a physically reasonable model for the nozzle requires that the width of the nozzle $\gtrsim 2r_g$. This is discussed in Section 4.3.

The second physical scale of interest is the period of gyration, T_g. From equation (131),

$$\omega' = \frac{qB}{m_0 q} = \frac{2\pi}{T_g'}, \tag{135}$$

where the dashed quantities refer to the comoving frame. In the laboratory frame, relativistic time dilation implies

$$T_g = \gamma T_g'. \tag{136}$$

If we substitute equations (23) and (136) into equation (135) we obtain

$$T_g = \gamma^3 \frac{2\pi m_0}{qB} = \gamma^3 T_{g0}, \tag{137}$$

where T_{g0} is the non-relativistic period of gyration, where $T_{g0} = 2\pi m_0/qB$.

In Figure 8 we compare the numerical solution of equations (121) and (122) against the analytic solution of equation (137). This is done by plotting T_g (in units of seconds) versus γ. We find good agreement between both the numerical and analytic solutions.

Finally, we consider the length of gyration, l_g. This is the distance that a charged particle will travel during one period of gyration. We note that such a length scale will be composed of two parts. The first part consists of the diameter of gyration, $2r_g$, which will be subject to relativistic length dilation. The second part is the distance the guiding centre will move during one period of gyration. Thus

$$l_g \approx \frac{2r_g}{\gamma} + \frac{E}{B} T_g. \tag{138}$$

As can be seen from Figure 9, equation (138) agrees relatively well with the numerical solutions obtained from equations (121) and (122).

References

Ardavan, H. 1976, ApJ, 203, 226
Battaner, E. 1996, Astrophysical Fluid Dynamics (Cambridge: Cambridge University Press)
Blackman, E. G., & Field, G. B. 1993, Phys. Rev. Lett., 71, 3481
Camenzind, M. 1990, in Accretion and Winds, Reviews in Modern Astronomy 3, ed. G. Klare (Berlin: Springer-Verlag), 234
Chow, E., & Monaghan, J. J. 1997, J. Comp. Phys., 134, 296
Contopoulos, J. 1995, ApJ, 450, 616
Ducati, A. C., Giannini, G. M., & Muehlberger, E. 1964, AIAA Journal, 2, 1452
Ellis, G. F. R., & Williams, R. M. 1988, Flat and Curved Space–Times (Oxford: Clarendon Press)
Goldreich, P., & Julian, W. H. 1970, ApJ, 160, 971
Hughes, W. F., & Brighton, J. A. 1991, Schaum's Outline Series, Theory and Problems of Fluid Dynamics (New York: McGraw-Hill)
Jahn, R. G. 1968, Physics of Electric Propulsion (New York: McGraw-Hill)
Kennel, C. F., Fujimura, F. S., & Okamoto, I. 1983, Geophys. Ap. Fluid Dyn., 26, 147
Khanna, R. 1998, MNRAS, 294, 673
Koide, S., Nishikawa, K.-I., & Mutel, R. L. 1996, ApJ, 463, L71
Landau, L. D., & Lifshitz, E. M. 1975, The Classical Theory of Fields (Oxford: Butterworth-Heinemann)
Landau, L. D., & Lifshitz, E. M. 1997, Fluid Mechanics (Oxford: Butterworth-Heinemann)
Liffman, K., & Siora, A. 1997, MNRAS, 290, 629
Liffman, K. 1998, PASA, 15, 259
Martí, J. M^{a}., & Müller, E. 1996, J. Comp. Phys., 123, 1
Melatos, A., & Melrose, D. B. 1996, MNRAS, 279, 1168
Michel, F. C. 1969, ApJ, 158, 727
Mirabel, I. F., & Rodriguez, L. F. 1998, Nature, 392, 673
Morozov, A. L., & Solov'ev, L. S. 1980, in Reviews of Plasma Physics, Volume 8, ed. M. A. Leontovitch (New York: Consultants Bureau), 1
Morozov, A. I. 1990, Sov. J. Plasma Phys., 16, 69
Pai, S.-I. 1962, Magnetogasdynamics and Plasma Dynamics (Vienna: Springer-Verlag)

https://doi.org/10.1071/AS01034 Published online by Cambridge University Press

Schoenberg, K., Gerwin, R., Barnes, C., Henins, I., Mayo, R., Moses Jr, R., Scarberry, R., & Wurden, G. 1991, American Institute of Aeronautics and Astronautics 91-3570
Sutton, G. W., & Sherman, A. 1965, Engineering Magnetohydrodynamics (New York: McGraw-Hill)
Thorne, K. S., & Macdonald, D. 1982, MNRAS, 198, 339
Weinberg, S. 1972, Gravitation and Cosmology: Principles and Applications of the General Theory of Relativity (New York: John Wiley and Sons)
Wolfram, S. 1996, The Mathematica Book, 3rd edition, Wolfram Media/Cambridge University Press

https://doi.org/10.1071/AS01034 Published online by Cambridge University Press